Research Article

Journal of Environmental Nanotechnology

Hybrid Nanofluid-based Thermal Energy Storage for Next-generation Concentrated Solar Power System

M. Rajagopal[1*], E. Stephena[2], S. V. Priya[2], A. Manigandan[3], J. Allen Jeffrey[3], AnilKumar[1] and S. Suresh Kumar[1]

[1]Department of Mechanical Engineering, PERI Institute of Technology, Chennai, TN, India
[2]Department of Electronics and Communication Engineering, Loyola Institute of Technology, Chennai, TN, India
[3]Department of Mechanical Engineering, Loyola Institute of Technology, Chennai, TN, India
Received: 23.12.2025 Accepted: 07.02.2026 Published: 30.03.2026
*mrajagopal1973@gmail.com

ABSTRACT

This study presents an experimental analysis of thermal energy storage (TES) system at high temperatures combined with a parabolic trough solar collector. The system utilizes solar salt ($NaNO_3$–KNO_3 eutectic) for thermal storage and a graphene–TiO_2/ethylene glycol hybrid nanofluid as the heat transfer medium. The main aim is to assess the impact of the hybrid nanofluid on the charging and discharging performance in outdoor solar operating conditions. A 100-L TES tank with 360 sealed solar saltmodules was charged with an average thermal input of 2.3 kW provided by the solar collector. The temperature changes along the axis during charging and discharging were tracked with several thermocouples. The findings demonstrate enhanced heat transfer during charging, decreased thermal layering close to the melting point of solar salt, and prolonged heat-release time during discharging with the application of the hybrid nanofluid. The system's charging efficiency, discharging efficiency, and round-trip efficiency were 48.6%, 81.6%, and 39.6%, respectively. The results indicate the capability of hybrid nanofluid-assisted heat transfer to improve the thermal performance of molten-salt-based TES systems used in concentrated solar powerapplications.

Keywords: Hybrid nanofluid; Parabolic trough collector; Thermal energy storage; Graphene–TiO_2 nanoparticles; Solar salt.

1. INTRODUCTION

A potential renewable energy technology that can store thermal energy during sunshine and release it for use during periods of low solar radiation is Concentrated Solar Power (CSP) system. However, the efficiency of these systems is largely dependent on how well their Thermal Energy Storage (TES) units work. Currently, two-tank molten salt systems using a eutectic combination of sodium nitrate and potassium nitrate ($NaNO_3$–KNO_3) are used in the majority of commercial CSP facilities. These salts are appealing because they are reasonably priced and thermally stable at high temperatures. Their limitations, however, particularly their poor thermal conductivity (about 0.5 W/mK) and modest specific heat capacity (~1.5 kJ/kgK), limit heat transfer rates and overall storage efficiency. As a result, charging and discharging operations are slower, and round-trip efficiency in CSP systems is reduced.

Among various molten salts, solar salt, a binary mixture of sodium nitrate and potassium nitrate, has emerged as a widely adopted sensible heat storage medium in CSP plants (Bradshaw and Meeker, 1990). Recent research indicate that the thermal efficiency of solar thermal systems can be augmented by employing nanofluids as heat transfer fluids (HTFs), due to their superior effective thermal conductivity and convective heat transfer properties (Eastman *et al.* 1996). Metal oxide nanoparticles, including TiO_2, have demonstrated stable dispersion and advantageous thermophysical characteristics for high-temperature heat transfer applications (Saidur *et al.* 2011; Mahian*et al.*2013). Graphene-based hybrid nanofluids, in particular, have shown promising potential for solar thermal and CSP-related applications due to their high intrinsic thermal conductivity and improved dispersion behavior.

In a conventional concentrated solar power system, the thermal energy storage medium and the heat transfer fluid serve distinct yet complementary functions. Molten nitrate salts, such as solar salt, are frequently utilized as thermal storage media due to their thermal stability and capacity for storage, while separate heat transfer fluids are necessary to effectively convey solar heat from the collector to the storage unit. Consequently, the efficacy of the thermal energy storage system is dependent not only on the storage material but also on the thermophysical characteristics of the circulating heat transfer fluid.

Nanofluid technology has been investigated as a potential solution to these constraints in recent years. Heat transfer behaviour and thermal conductivity are

known to be greatly improved by nanofluids, which are made up of nanoparticles suspended in a traditional heat transfer fluid. Research employing oxide nanoparticles such as Al_2O_3, CuO, and TiO_2, as well as carbon-based nanostructures, has demonstrated considerable increases in both heat transfer coefficients and overall thermal performance. Among them, hybrid nanofluids have received considerable interest because they can utilize the capabilities of distinct materials. While carbon-based materials like graphene give extraordinarily high inherent heat conductivity, metal oxides offer endurance and thermal stability.

In CSP systems employing parabolic troughs, the heat transfer fluid experiences cyclic thermal stress, substantial heat flux, and high operational temperatures; consequently, both thermal stability and improved heat transfer properties are essential. Hybrid nanofluids, which integrate carbon-based nanostructures with metal oxides, are thus being investigated for CSP–TES applications, given their potential to provide a compromise between elevated thermal conductivity, stable dispersion, and reliable performance under solar thermal operating conditions.

For laboratory-scale experimental investigations, ethylene glycol is frequently adopted as a base fluid for nanofluid formulation due to its chemical stability, compatibility with nanomaterial dispersion techniques, and suitability for controlled thermophysical characterization. In the present study, ethylene glycol is employed as a surrogate heat transfer fluid to evaluate the thermal influence of hybrid nanofluids under representative temperature ranges, rather than as a direct replacement for commercial CSP heat transfer oils or molten-salt HTFs.

Despite encouraging development, experimental investigations that integrate hybrid nanofluids with molten salt TES systems, especially under realistic solar charging conditions, remain restricted. There is a lack of experimentally proven hybrid nanofluid–salt combinations for CSP applications since the majority of current research either concentrates on numerical modelling or single-nanoparticle systems. The experimental assessment in this study was undertaken under outdoor solar settings utilizing a parabolic trough collector, with operating temperatures ranging from roughly 30 °C to 250 °C and multiple charging–discharging cycles to imitate actual solar thermal operation. In order to address the gap, the present work experimentally develops and characterizes a Graphene–TiO_2 hybrid nanofluid formulated in ethylene glycol solution. In order to evaluate the advantages of hybrid nanofluid integration for next-generation CSP thermal storage systems, this work focusses on estimating heat transfer characteristics, charging and discharging behaviour, and system-level performance, including energy efficiency.

Improving the effectiveness and dependability of thermal energy storage systems is directly associated with better harvest of solar energy and decreased dependence on fossil-fuel-based backup heating. Thus, improvements in TES performance aid in achieving wider energy sustainability goals and align with environmental initiatives aimed at lowering greenhouse gas emissions by utilizing renewable solar resources more efficiently.

This paper highlights the significance of hybrid nanomaterials in enhancing thermal energy storage performance in order to clearly link the work with nanoscale science and environmental nanotechnology. The nanoscale particles in the graphene nanoplatelet–TiO_2 hybrid nanofluid employed in this study (graphene platelets ~250 nm lateral dimension and TiO_2 nanoparticles ~25 nm) allow for better optical absorption, improved heat transfer behavior, and increased thermal conductivity. By lowering fossil fuel-based backup heating in solar thermal applications, these nanoscale interactions greatly improve TES charging/discharging performance and promote sustainable thermal energy consumption.

1.1 Current Developments in Thermal Energy Storage and Nanofluids

1.1.1 Thermal Energy Storage in CSP Systems

Thermal energy storage plays a vitalrole in CSP systems as it allows for the separation of solar energy collection from electricity generation, enhancing dispatchability and grid stability. Commercial CSP facilities mainly utilize two-tank molten salt storage systems that use a eutectic blend of sodium nitrate and potassium nitrate because of their thermal stability, affordability, and suitability for high-temperature operations (Gil *et al.* 2010). These salts generally function within a temperature span of 220–565 °C and deliver consistent performance throughout successive thermal cycles (Kuravi *et al.* 2013).

Techno-economic evaluations indicate that TES greatly improves the capacity factor of plants and lowers the levelized cost of electricity by providing consistent energy output during times of reduced solar irradiance. Comparative analyses of thermocline and dual-tank storage setups show enhanced system reliability and cost effectiveness when TES is well integrated (Cascetta *et al.* 2021). Nevertheless, the comparatively low thermal conductivity and average specific heat capacity of molten salts restrict heat transfer rates, leading to slower charging and discharging cycles and decreased round-trip efficiency. Rajagopal (2025) demonstrated that integrating PCMs within repurposed EV battery casings can deliver reliable thermal performance while avoiding virgin material consumption. District-heating studies also showed that modular latent heat storage units can

effectively reduce peak loads and improve flexibility, reinforcing the feasibility of battery-upcycling strategies. The study aligned with contemporary research emphasizing enhanced heat-transfer architectures in PCM-based storage units.

1.1.2 Nanofluids for Solar Thermal Heat Transfer

Nanofluids, which are suspensions of nanoparticles (1–100 nm) in standard base fluids, have surfaced as potential heat transfer media for solar thermal applications owing to their improved thermal conductivity, specific heat capacity, and convective heat transfer coefficients (Xiong *et al.* 2021). These enhancements lower thermal resistance between absorber surfaces and working fluids, resulting in increased heat absorption and diminished thermal losses. Studies in numerical and computational fluid dynamics indicate that the performance of nanofluids is significantly affected by factors such as nanoparticle concentration, particle size, flow conditions, and collector geometry. Optimization through simulation has enhanced solar collector designs, lowered development expenses, and aided integration with TES and hybrid renewable systems (Abbas *et al.*2019). Performance evaluations consistently indicate that nanofluids enhance overall energy conversion efficiency in comparison to traditional fluids (Alhamayani, 2024).

Experimental studies on parabolic trough collectors (PTCs) reveal notable efficiency enhancements when nanofluids substitute traditional fluids. For instance, CuO–water nanofluids have realized efficiency improvements greater than 50 % in comparison to water, mainly attributed to decreased radiative and convective losses (Ram *et al.*2023). In a similar way, metal oxide nanofluids mixed with thermal oils like Therminol VP-1, Therminol 75, and Syltherm-800 have demonstrated significant enhancements in thermal performance, emphasizing the significance of the thermophysical properties of the base fluid (Alhamayani *et al.*2024). Nanofluids have been assessed in high-flux receivers and different concentrator designs. Graphite nanofluids in minimal volume fractions have shown up to 10 % efficiency improvements in parabolic trough systems (Taylor *et al.*2011), whereas research on solar dish concentrators suggests that Al_2O_3 nanofluids enhance thermal efficiency, and CuO nanofluids deliver better exergy performance (Loni *et al.*2018). Thermodynamic evaluations further verify that nanofluids enhance exergy efficiency and decrease entropy production. SiC–water nanofluids, for instance, have shown substantial exergy improvements compared with pure water due to enhanced energy transport capability (Rajendran *et al.*2018).

1.1.3 Hybrid Nanofluids and Synergistic Heat Transfer Enhancement

Hybrid nanofluids, consisting of two or more types of nanoparticles, have attracted significant interest due to their ability to leverage the excellent thermal conductivity of carbon-based nanomaterials along with the thermal stability of metal oxides. This synergistic effect results in enhanced thermophysical properties in comparison to mono nanofluids (Suresh *et al.* 2012). Hybrid nanofluids based on graphene, especially those combining grapheme with metal oxides, display increased solar absorptivity, better dispersion stability, and elevated thermal conductivity. Experimental studies show considerable enhancements in collector efficiency and heat transfer rates with the application of hybrid nanoparticles. For instance, graphene–Fe_3O_4/water nanofluids have shown significant improvements in thermal efficiency attributed to the synergy of optical and thermal effects (Al-Rabeeah *et al.* 2024).

The incorporation of hybrid nanofluids and passive heat transfer enhancement methods like internal fins, metal foams, and turbulators has led to additional performance enhancements. Metal foam inserts boost effective thermal conductivity and heat transfer area, whereas turbulators improve mixing and disrupt the boundary layer (Heyhat *et al.* 2020). Integrated enhancement strategies have demonstrated greater efficiency improvements compared to standalone techniques, though at the expense of higher pressure drop and pumping power demands (Bellos *et al.* 2018; Esmaeili *et al.* 2023). Comparative studies indicate that the choice of base fluid is essential in affecting the performance of hybrid nanofluids. Research on Syltherm-800 and Therminol VP-1 demonstrates that the thermophysical compatibility of nanoparticles with the base fluid greatly affects the overall efficiency of the collector (Brahim and Jemni, 2023).

1.1.4 Integration of Nanofluids with CSP and TES

The incorporation of nanofluids in CSP systems has been examined at both the component and plant scales. Heat transfer loops utilizing nanofluids have shown increased heat absorption by receivers, minimized irreversibility, and improved overall energy conversion efficiency in solar thermal power facilities (Ghasemi and Ranjbar, 2017). In solar-powered trigeneration systems, nanofluids enhance the efficiency of thermal energy usage across various output streams, boosting overall system performance (Bellos and Tzivanidis, 2017). Comparative analyses of various collector technologies suggest that Fresnel reflector systems utilizing nanofluids may surpass traditional PTCs regarding energy, exergy, and entropy efficiency (Huang *et al.*2020). Economic assessments indicate that Al_2O_3–water nanofluids present a reduced levelized cost of energy, while CuO-based nanofluids face elevated costs due to the price of

nanoparticles, highlighting the necessity for techno-economic optimization.

In the TES interface, the use of high-conductivity nanofluids with molten salt storage boosts heat exchange rates, resulting in quicker charging–discharging cycles and increased storage efficiency (Alva *et al.* 2017). Thermodynamic evaluations at the plant level verify enhanced heat gain in receivers and decreased entropy generation with the use of nanofluids.In spite of these developments, the majority of current research concentrates on numerical modelling or single nanofluid systems. Research studies on hybrid nanofluids combined with molten salt thermal energy storage under actual solar operational conditions are still scarce. This gap emphasizes the necessity for systematic experimental assessment of hybrid nanofluid–TES integration in PTC-based CSP systems.

1.2 Environmental Nanotechnology Perspective

By showing how nanoscale additions might improve thermal storage based on renewable energy, the current study advances the field of environmental nanotechnology. In solar-powered TES systems, hybrid graphene–TiO_2 nanoparticles enhance sunlight absorption, speed up heat transfer, and shorten charging times. A sustainable substitute for traditional fossil-based heating, the resulting energy savings directly translate into lower CO_2 emissions. Thermal oxidation analysis was used to confirm the environmental resilienceof the nanoparticles, guaranteeing their suitability for long-term use in high-temperature solar plants. Therefore, the proposed nano-enhanced TES framework combines environmental effect mitigation, high-temperature energy conversion, and nanomaterials.

The significance of this study for CSP applications is demonstrated by examining quantifiable operating conditions, such as high-temperature operation, exposure to actual solar flux, and repetitive thermal loading. These elements are essential for evaluating the actual efficiency of TES and HTFs in genuine solar thermal operating conditions.

2. METHODOLOGYAND EXPERIMENTAL INVESTIGATION

This work combines the formulation and characterisation of a Graphene–TiO_2 hybrid nanofluid with the development and testing of a solar-driven TES system utilizingsolar salt as the thermal energy storage material. All studies were carried out under regulated and repeatable settings to correctly measure the thermophysical behaviour of the hybrid nanofluid and its influence on the overall thermal performance of the TES system.In the current experimental setup, the graphene–TiO_2 hybrid nanofluid operates solely as a HTF moving through the parabolic trough collector circuit. The solar salt is contained within the thermal energy storage tank and does not directly interact with the nanofluid. Heat energy is conveyed from the HTF to the storage medium indirectly *via* designed heat transfer surfaces, ensuring material compatibility and avoiding chemical interaction between the nanofluid and molten salt.

2.1 Preparation of the Graphene–TiO_2 Hybrid Nanomaterial Preparation and Dispersion Procedure

Ethylene glycol was chosen as the base fluid for the hybrid nanofluid formulation to enable regulated laboratory-scale testing. Its consistent thermophysical properties, ability to disperse nanoparticles, and appropriateness for high-temperature analysis render it a commonly utilized surrogate HTF in solar thermal experimental research. The employment of ethylene glycol in this study is not meant to symbolize a commercial CSP heat transfer fluid, but instead to facilitate a systematic assessment of the heat transfer enhancement caused by nanomaterials under typical temperature conditions.

A two-step dispersion method was used to prepare the hybrid nanofluid. The base fluid, ethylene glycol (EG), was used to scatter graphene and TiO_2 nanoparticles in equal mass amounts (50:50). Graphene nanoplatelets (GNPs) and titanium dioxide (TiO_2), two manufactured nanomaterials with nanoscale dimensions (GNP thickness < 10 nm; TiO_2 particle size = 20–30 nm), are both present in the hybrid nanofluid. Four concentrations (0.05, 0.10, 0.15, and 0.20 weight percentage) were prepared by properly weighing and mixing the nanoparticles. Each combination was subjected to 2 hours of ultrasonication at 40 kHz in order to guarantee steady and consistent suspension. No surfactants were used since the goal was to ensure chemical compatibility with solar salt during high-temperature operation and to avoid unwanted reactions during thermal cycling. Stability was evaluated using visual sedimentation monitoring over a 72-hour period and zeta potential tests, all of which were above 32 mV. The hybrid nanofluid maintained a stable dispersion appropriate for high-temperature heat transfer applications, according to both evaluations.

2.1.1 Nanomaterial Stability Evaluation

Zeta potential analysis was used to systematically assess nanofluid stability. The results consistently showed values above +32 mV, showing significant electrostatic repulsion between dispersed nanoparticles and, as a result, a low tendency for agglomeration. It is generally acknowledged that this zeta potential barrier is necessary for stable colloidal suspensions, particularly when subjected to heat loading. A 72-hour visual sedimentation test was conducted under

quiescent conditions to supplement the electrokinetic evaluation. Throughout the observation time, there was no discernible settling, layering, or particle clustering, indicating that the hybrid Graphene–TiO_2 nanoparticles remained evenly suspended without the requirement for surfactants. The hybrid nanofluid's exceptional resistance to sedimentation was confirmed by the stability being maintained for all tested concentrations up to 0.20 weight percent. For high-temperature thermal systems, this stability is essential because it guarantees constant thermophysical characteristics, avoids flow loop obstructions, and promotes long-term operational dependability in solar-thermal energy storage applications.

2.2 Physicochemical Characterization of Nanomaterials

The hydrodynamic particle size distribution was obtained using Dynamic Light Scattering (DLS), which verified that graphene and TiO_2 nanoparticles remained in the nanoscale range even after extended ultrasonication. A Malvern Zetasizer Nano ZS was used to test the zeta potential, and the results consistently surpassed ±30 mV, suggesting low aggregation and good electrostatic stability. The existence and homogeneous distribution of both nanoparticles inside the ethylene-glycol base fluid were confirmed by identifying the distinctive optical absorption peaks of graphene and TiO_2 using UV-visible spectroscopy. In order to determine if GNPs, TiO_2, and the hybrid nanofluid are suitable for CSP operating temperatures, Thermogravimetric Analysis (TGA) was also performed up to 600°C to evaluate their thermal stability and oxidation resistance.

2.3 Measurement of Thermo-physical Properties

Thermo-physical properties such as thermal conductivity, specific heat capacity, viscosity, and density of the hybrid nanofluid were tested to establish its appropriateness for CSP-scale TES systems. Thermal conductivity was measured using a Hot Disk TPS 2500 S instrument, Differential Scanning Calorimetry (DSC) was used to analyze the nanofluid's specific heat capacity in order to assess nanoscale thermal interactions and quantify the improvement in energy storage capacity. Additionally, the viscosity of the samples was evaluated using a high-temperature rotary viscometer.

2.3.1 Thermal Conductivity Behavior

Fig. 1 depicts how temperature (ranging from 20 to 250 °C) and the concentration of nanoparticles (from 0 to 0.20 wt.%) affect the thermal conductivity of the graphene–TiO_2/ethylene glycol hybrid nanofluid.

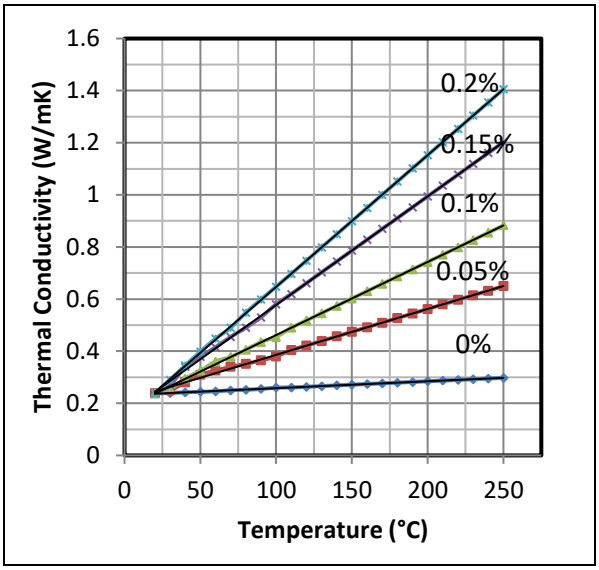


Fig.1: Variation of thermal conductivity with temperature and nanoparticle concentration

Thermal conductivity measurements showed a constant rise with temperature and concentration of nanoparticles. Even the smallest amount (0.05 weight percent of nanoparticles) produced a noticeable improvement as compared to pure ethylene glycol. The 0.20 weight percent sample had the greatest increase at 250°C due to the synergistic effects of graphene's extraordinarily high intrinsic heat conductivity and excellent dispersion stability of TiO_2. The whole increase was ascribed to improved micro-convection, percolation networks, and interfacial heat transfer. Micro-convection denotes localized fluid movement caused by the Brownian motion of suspended nanoparticles, which can enhance energy transfer at the microscale and lead to better effective thermal conductivity. Percolation networks illustrate the development of linked thermally conductive routes formed by high-aspect-ratio or high-conductivity nanoparticles, like graphene, allowing enhanced heat transfer within the fluid matrix. These mechanisms have been extensively documented as contributing elements to thermal improvement in hybrid nanofluids.

2.3.2 Specific Heat Capacity Behavior

Fig. 2 underscores the changes in specific heat of the hybrid nanofluid as the temperature rises from 20°Cto 250°C. The specific heat capacity increased in direct proportion to particle concentration and inversely proportion to the temperature. The ability of the nanoparticles to store additional energy through surface interactions and to facilitate more effective energy transfer within the fluid is responsible for this rise. At moderate-to-high temperatures, the 0.15–0.20 weight percent nanofluids showed the highest specific heat capacities, which improved the fluid's ability to retain energy during sensible heating.

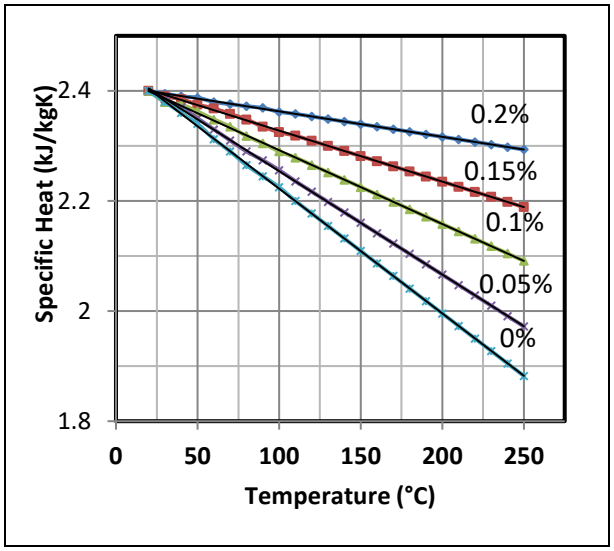


Fig. 2: Variation of specific heat with temperature and nanoparticle concentration

2.3.3 Viscosity Behavior

Fig. 3 illustrates the viscosity characteristics of the hybrid nanofluid throughout the temperature span of 20 to 250 °C. Viscosity significantly reduced with temperature, which is beneficial for circulating at high temperatures. The addition of nanoparticles somewhat increases the viscosity at lower temperatures, but the change was significantly less at higher temperatures. By 250 °C, viscosity values for all concentrations converged to levels suitable for effective fluid transport in solar thermal systems.

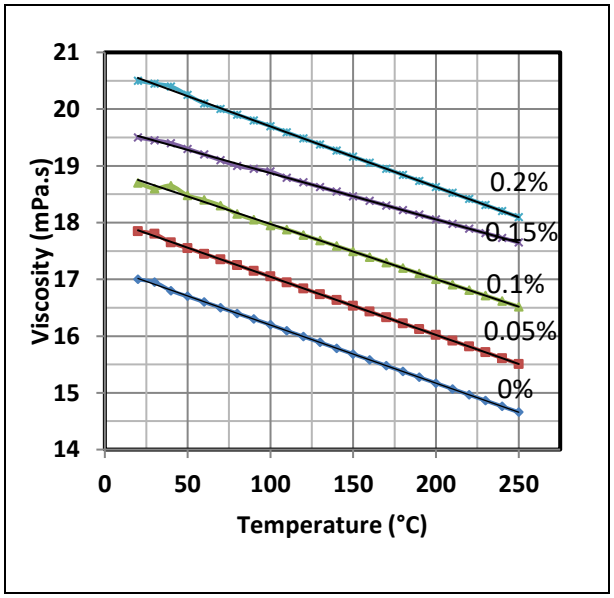


Fig. 3: Variation of viscosity with temperature and nanoparticle concentration

All of these experiments show that the hybrid nanofluid provides more specific heat and better thermal conductivity while keeping a suitable viscosity between 20 and 250 °C, which are essential characteristics for effective TES charging and discharging. While specific system parts might have greater theoretical temperature limits, the operating temperature of the hybrid nanofluid in all experimental trials was kept within roughly 30 to 250 °C. This range aligns with the recorded inlet and outlet temperatures of the HTF during solar charging and discharging tests.

2.4 Environmental Relevance of the Nanomaterial

The hybrid graphene–TiO_2 nanomaterial allows for more efficient utilization of renewable solar energy and improves solar-to-thermal conversion efficiency. Its use with molten-salt TES lowers emissions intensity, lessens dependency on fossil fuel-based heating, and advances long-term sustainability objectives. Because the nanoparticles are non-volatile, chemically stable, and integrated into a closed-loop system, the dangers of environmental exposure are reduced.

2.5 Thermo-physical Properties of Solar salt

Solar salt (60:40 $NaNO_3$–KNO_3) was selected as the PCM due to its melting point of around 220 °C and its thermal stability up to roughly 560 °C. It possesses a moderate specific heat capacity (1.0–1.6 kJ/kgK), a high latent heat of fusion (180–200 kJ/kg), and little volume change during phase transition. Its low molten-state viscosity and thermal conductivity (0.45–0.7 W/mK) provide effective heat transmission and natural convection inside the TES tank. For the purposes of experimental analysis, solar salt is regarded as a sensible heat thermal energy storage medium, aligning with its thermophysical properties detailed in the literature. All temperature readings were taken with calibrated K-type thermocouples having an uncertainty of ±0.5 °C. Flow rate and irradiation measurements were captured using instruments specified by the manufacturer, and all reported figures represent average experimental data unless mentioned otherwise.

2.6 Experimental Setup

A high-temperature TES test bed was developed to investigate the charging and discharging performance of the hybrid nanofluid–solar salt combination. The experimental setup consists of four primary parts such as a PTC, a receiver and fluid circulation loop, a PCM-based TES tank, and an integrated instrumentation and data acquisition system. Fig. 4 shows the block diagram of the experimental setup and Fig. 5 shows the schematic diagram of the experimental setup. While some system elements like piping, pumps, and insulation materials can handle higher temperatures, the hybrid nanofluid functioned within a managed temperature range of about 30 to 250℃ throughout all experimental trials. The

recorded temperatures align with measured values within this operational range.

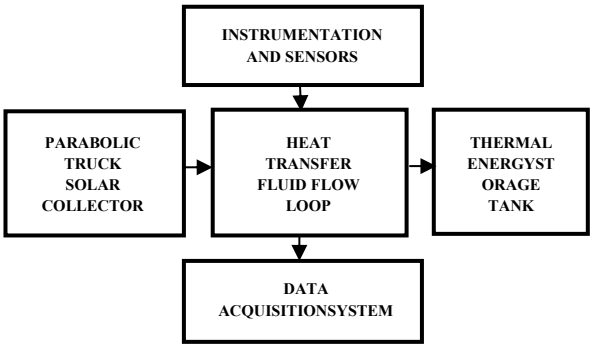


Fig. 4: Block diagram of the experimental setup

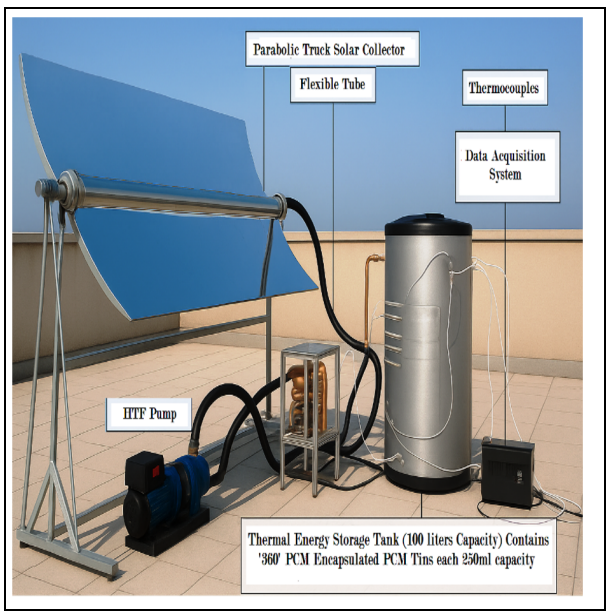


Fig. 5: Schematic of the experimental setup

2.6.1 Parabolic Trough Solar Collector

The parabolic trough collector has 1.8-m long and it supply the thermal input to the TES tank during charging period. The collector was installed on a steel frame with a north–south alignment and manually adjusted at every 30 minutes based on direction of solar rays to ensure appropriate orientation. High-reflectivity aluminium sheets (ρ = 0.90–0.92) were used to build the reflecting surface, which was intended to concentrate incoming solar energy along the linear focal axis of the trough.At the focal line, a stainless-steel (SS-316) absorber tube with a 25-mm diameter and selective coating collected the focused solar radiation. The absorber tube was covered with a borosilicate glass envelope to prevent heat loss from radiation and convection. The system continuously received direct normal irradiance (DNI) in the range of 850–950 W/m² while the sky was clear, allowing the PTC to provide the circulating hybrid nanofluid with about 2.5–3.0 kW of thermal power. After absorbing heat, the fluid was routed to the TES tank to commence PCM charge.

2.6.2 Thermal Energy Storage Tank

The 100-liter vertically orientated cylindrical TES tank was made of stainless steel (SS-316) and designed to handle high temperatures and corrosive molten-salt conditions. The tank was insulated externally with a 50-mm thick layer of ceramic wool and aluminium cladding to minimize heat losses during operation. The PCM was solar salt, which was contained in 360 tins, each 250 mL capacity and made of tin-plate. There was 0.2 kg of solar salt in each tin. Inside the tank, these PCM modules were arranged in four vertical rows, each containing ninety tins. This configuration increases the surface area for heat transfer, encourages uniformity in melting and solidification, and provides a strong geometric structure for multiple thermal cycles. The TES tank had 72 kg of PCM in total.

Tin-plate encapsulation was chosen for the solar salt modules because of its accessibility, simple manufacturing process, and sufficient thermal conductivity for laboratory-scale testing. It is recognized that tin-plate materials could exhibit long-term corrosion or durability challenges when subjected to prolonged high-temperature molten-salt exposure. Nevertheless, the material was considered appropriate for controlled experimental assessment within the parameters and timeframe of the current study.

2.6.3 Thermocouple Network

Eight K-type thermocouples were installed along the tank's height to track axial temperature variations during charging and discharging. The temperature of PCM was measured using four thermocouples, and the temperature of heat transfer fluid was measured using an additional four thermocouples. These sensors provided information on thermal stratification, melting advancement, and heat distribution by recording temperatures at the bottom, lower-middle, upper-middle, and top sections of the tank. Each thermocouple was calibrated using a dry-block calibrator to achieve a measurement accuracy of ±0.5 °C in order to ensure reliable data gathering during high-temperature operation.

The thermocouples were placed axially throughout the height of the thermal energy storage tank at specific points, covering the bottom (0.5m from middle), lower-middle (0.25m from Middle), upper-middle (0.25m from middle), and top sections (0.5m from middle, maintaining uniform spacing between neighboring sensors. Each thermocouple was placed into the storage medium via specific guide sleeves to a predetermined depth, guaranteeing the measurement of core temperatures of the solar salt instead of surface or

wall temperatures. This insertion technique reduces wall conduction impacts and ensures dependable observation of the internal thermal dynamics of the storage medium.

2.6.4 Hybrid Nanofluid Circulation Circuit

A gear pump that could handle temperatures as high as 600°C drove the nanofluid through a high-temperature flow loop. A double-pipe heat exchanger between the PTC and TES tank, insulated SS-316 pipes, and a high-temperature flowmeter were all part of the loop. These components ensured consistent fluid circulation and precise control of heat input during charging and discharging.A high-temperature closed-loop flow circuit was used to circulate the hybrid nanofluid. The loop included insulated SS-316 pipelines for thermal durability, a double-pipe heat exchanger between the PTC outlet and the TES tank for temperature control, a variable-speed gear pump that can handle operating temperatures up to 600 °C, and a high-temperature flowmeter to measure mass flow rate in real time. This circuit enabled consistent fluid circulation during charging and discharging process and stable, controlled heat transfer, enabling accurate assessment of TES performance.

The heat exchanger used in this system was crafted to enable indirect heat transfer between the hybrid nanofluid flowing through the parabolic trough collector loop and the solar salt housed in the thermal energy storage tank. The two operational mediawere hydraulically and physically separated, with thermal energy conveyed exclusively through metallic heat transfer interfaces. This setup avoids direct interaction between the nanofluid and the molten salt, guaranteeing compatibility of materials and regulated thermal exchange.

2.6.5 Data Acquisition System

Temperatures at every thermocouple point, the collector and TES tank's intake and outlet temperatures, real-time solar irradiation, nanofluid flow rate, and heat flux at the receiver were all continuously recorded by a data acquisition system. Data were acquired at a frequency of 1 Hz using a LabVIEW interface, providing high-resolution insight into transient thermal behaviour throughout charging and discharging cycles. The combination of solar salt PCM, hybrid nanofluid HTF, and high-flux PTC configuration provided a realistic and comprehensive platform for evaluating TES performance under genuine solar operating conditions. Temperature measurements were taken with calibrated K-type thermocouples that have an uncertainty of ±0.5 °C. Data was collected at a constant sampling rate, and the values presented are actual measurements without numerical smoothing unless specified otherwise.

2.7 Solar Collector-based Heating Method

The PTC served as the primary heating source for the TES charging experiments, which ran from 9:00 AM to 3:00 PM. After being pumped through the absorber tube, the hybrid nanofluid immediately transferred heat to the solar salt in the tank by absorbing concentrated solar energy. Direct normal irradiance consistently fluctuated between 850 and 950 W/m^2, providing steady high-intensity heat input and manual tracking allowed for optimal sun alignment.

2.7.1 TES Charging Procedure

The PCM modules and hybrid nanofluid were both allowed to reach an initial temperature of about 30 °C prior to each charging attempt. After that, charging was done continuously in the sun for six hours. Eight axially positioned thermocouples recorded temperature changes at each layer of the tank to track heat penetration, stratification, and the start of melting. Charging continued until PCM temperatures above the PCM melting point (~220 °C), indicating substantial melting in the upper region.

2.7.2 TES Discharging Procedure

Discharging was started by running a cooler working fluid through the heat exchanger once the PCM reached a steady post-charging temperature of around 221 °C. The entire discharge process took 360 minutes. Axial temperatures were continuously recorded in order to characterize latent heat release, PCM solidification behaviour, and thermal retention performance. The basis for analyzing the discharge efficiency of the TES system was provided by these data.

2.8 Performance Evaluation and Data Analysis

The following key performance indicators were computed:

Heat Transfer Rate: $Q = \dot{m}C_p(T_{in} - T_{out})$

Charging Efficiency: $\eta_{charge} = \frac{Q_{stored}}{Q_{input}}$

Discharging Efficiency: $\eta_{discharge} = \frac{Q_{useful}}{Q_{stored}}$

Round-Trip Efficiency: $\eta_{RT} = \eta_{charge} \times \eta_{discharge}$

These indicators were used to measure the TES system's performance.

3. RESULTS AND DISCUSSION

3.1 Charging Behaviour

The temperature history of the four axial layers during the course of the six-hour charging time is shown in Fig. 6. At around 30 °C, the entire tank was almost isothermal at first. During the first hour, the top and upper-middle layers heat up significantly quicker than the bottom areas because they receive direct thermal input from the entering hot nanofluid. After 60 minutes, there is a distinct gradient in the temperature distribution, with the top layer reaching around 72 °C, the upper-middle layer about 66 °C, the lower-middle layer about 58 °C, and the bottom layer about 52 °C.

This stratification is characteristic of thermal storage systems and exhibits convection-dominated heating at the fluid inflow and conduction-dominated heating deeper inside the TES tank. All layers exhibit a consistent temperature increase between 60 and 180 minutes, and the temperature differentials between layers start to narrow. There is a clear vertical temperature gradient at 180 minutes, with temperatures reaching around 167 °C at the top, 151 °C in the upper-middle region, 137 °C in the lower-middle region, and 123 °C at the bottom.

Improved axial heat penetration and increased internal convection inside the solar salt modules are shown by this decrease in the vertical temperature gradient. The top region reaches 222 °C, the upper-middle layer 221°C, the lower-middle layer 214 °C, and the bottom layer 191 °C after 300 minutes, suggesting almost uniform heating in the higher parts and a slightly lower temperature at the bottom. While the bottom layers continue to absorb sensible heat, melting starts in the upper region first. At the end of the charging process, the temperatures are almost consistent, with the top at 225 °C, the upper-middle at 224 °C, the lower-middle at 222 °C, and the bottom at 221 °C. This shows that solar salt is completely melted in all regions.

Despite solar salt experiencing a phase transition within a limited temperature range, the thermal energy storage characteristics seen in these experiments are mainly sensible. Any observable temperature plateaus are affected by heat transfer resistance, the geometry of encapsulation, and temporary charging conditions instead of by theoretical latent heat storage dynamics. The increased charging rates noted with the hybrid nanofluid can be linked to the better effective thermal conductivity and convective heat transfer properties documented for graphene–metal oxide nanofluids in previous research (Suresh *et al.* 2012). These mechanisms are considered as contributing elements instead of being directly measured phenomena in the current experimental study.

Because of the temperature disparities between the solar salt and the entering HTF, thermal stratification is considerable during the early charging period. Higher temperatures encourage buoyancy-driven convection within the molten solar salt; improved heat transfer from the hybrid nanofluid reduces axial temperature differences; the upper layers quickly approach the melting point and latent heat absorption moderates further temperature rise; and heat gradually diffuses downward, reducing variation between layers. These mechanisms all contribute to the weakening of the thermal stratification as charging proceeds.

The charging findings show that the hybrid nanofluid effectively transfers heat to the top solar salt layers, with a notable improvement in heat penetration following two to three hours of solar input. As a result, stratification steadily decreases as the system gets closer to thermal equilibrium, whereas solar salt melting starts at the top and moves downward. Overall, the charging behaviour of the TES unit is reliable and predictable, making it appropriate for CSP-scale operation.

The decrease in thermal stratification and the increase in heat penetration seen during hybrid nanofluid operation exemplify paired effects of enhanced convective and conductive heat transfer in the system. Consequently, these results are analyzed collectively as signs of enhanced thermal transport efficiency instead of distinct qualitative impacts. Although the experimental findings show quantifiable performance enhancements at the lab level, directly applying these results to large-scale concentrating solar power systems needs further study. Aspects like long-term stability, material compatibility, and system integration impacts were not included in the current study's focus.

3.2 Discharging Behaviour

The discharge profiles of the TES tank employing the hybrid nanofluid and the solar saltare shown in Fig.7. All axial layers begin at roughly 221 °C, suggesting consistent temperature distribution after charging. The noted enhancement in discharge behavior indicates a relative performance boost within the examined operating range and experimental setup. These findings should not be viewed as definitive performance boundaries or as representative of optimized system functioning outside the current experimental circumstances.

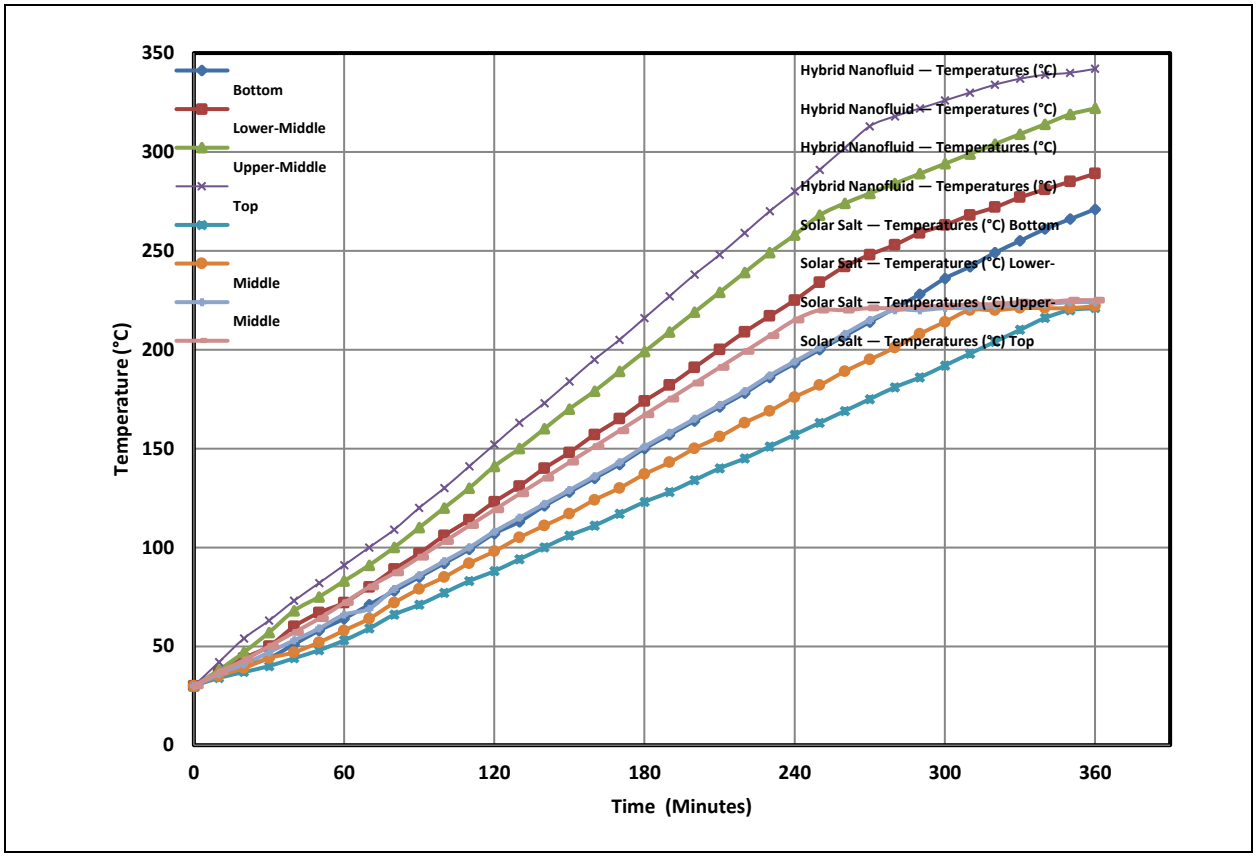


Fig. 6: Temperature distribution in TES tank during charging for solar salt and hybrid nanofluid

3.2.1 Initial Temperature Decline and Cooling Front Formation

Once the cool working fluid begins circulating, the temperature at the top of the tank lowers first since it is in direct thermal contact with the incoming cooling stream. Due to its greater thermal diffusivity and heat-carrying capacity, the hybrid nanofluid exhibits a shorter temperature drop than solar salt. A clear cooling front forms from top to bottom. In solar salt-based TES systems, this pattern (early heat release from the top layers, delayed cooling of the lower layers, and sequential, layer-by-layer energy extraction) is expected.

3.2.2 Latent Heat Release

One significant feature of the discharge curve is the latent heat plateau, which may be seen within the first 60 to 90 minutes. In this region, heat is released at a nearly constant temperature, the solar salt changes from liquid to solid, and the temperature progressively decreases. A longer plateau length, a more stable temperature profile, and more effective heat extraction from the energy storage material are all characteristics of the hybrid nanofluid. These benefits result from the nanofluid's ability to maintain a high heat transfer rate during phase change and reduce thermal resistance. The basic solar salt, on the other hand, discharges more quickly, indicating a higher level of latent heat depletion.

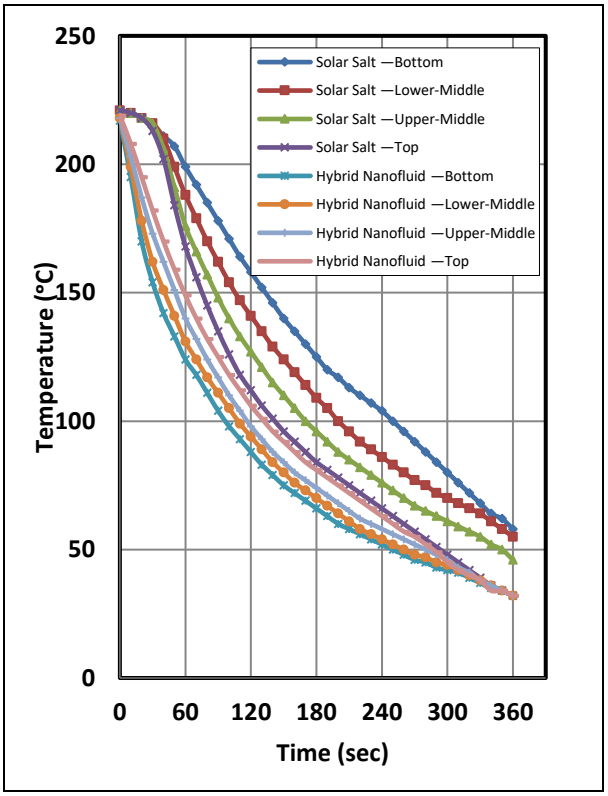


Fig.7: Discharging temperature profile in TES tank for solar salt and hybrid nanofluid

3.2.3 Sensible Cooling Stage

After the PCM has fully formed, the system enters the sensible cooling phase. At this point, the temperature drops faster, cooling becomes conduction-controlled, and any residual sensible heat is gradually eliminated. The hybrid nanofluid retains its higher temperatures, slower cooling rates, and longer usable discharge time even in this regime. These results are consistent with improved heat retention and more efficient energy extraction.

The combined charging and discharging results show that the graphene–TiO_2 hybrid nanofluid improves heat transfer during charging, decreases the time required to reach melting conditions, promotes uniform heat distribution, enhances latent heat recovery, slows down temperature decay during discharging, and increases the effective duration of heat delivery. Because of these qualities, the hybrid nanofluid is a great option for CSP thermal storage systems that need effective heat cycling and high-temperature stability.

3.3 Thermal Energy Stored During Charging

The sensible heat obtained while the material was heated from its starting temperature of 30 °C to 221 °C. The melting point of the eutectic mixture was used to determine the thermal energy retained by 72 kg of solar salt during the charging process. With a temperature increase of 191 °C and an average specific heat capacity of around 1.2 kJ/kgK for solid solar salt, the sensible heat storage was computed using Q_{SH} = mCpΔT. The quantity of thermal energy stored before melting began was determined to be around 16.5 MJ.

Latent heat storage was calculated using Q_{LH} = m × Latent heat. The quantity of thermal energy stored during melting was determined to be around 12.9 MJ.

3.4 Heat Discharging Rate of PCM

The heat discharge rate exhibits a characteristic three-stage pattern:

- **Rapid Initial Cooling:** Brought on by a large temperature differential between the PCM and the incoming coolant.
- **Latent Heat Extraction Stage:** A plateau where solidification takes place at a temperature that is almost constant Heat extraction rate, latent heat release duration, and PCM–HTF thermal coupling are all enhanced by the hybrid nanofluid.
- **Last Sensible Cooling:** Until the PCM is entirely solid, heat transfer becomes conduction-dominated, accelerating cooling.

During these stages, the hybrid nanofluid consistently displays the following properties: longer discharge times, higher retention temperatures, and slower cooling. Slight differences in temperature profiles and performance indicators across multiple experimental trials are ascribed to variations in solar irradiation and environmental factors.

3.5 Nano-enhanced Heat Transfer Mechanisms

Because of nanoscale phenomena such as greater thermal diffusivity, increased micro-convection around nanoparticles, and better thermal conductivity, the hybrid nanofluid exhibits superior thermal performance. Faster heat absorption in the PTC receiver and more effective heat transmission to the TES tank are made possible by the high intrinsic conductivity of graphene and the potent scattering ability of TiO_2 nanoparticles. Additionally, these nanoscale interactions enhance charging uniformity and lessen thermal stratification, demonstrating the critical role of nanotechnology in raising high-temperature TES efficiency.

3.6 Overall Thermal Performance Evaluation

The key performance metrics are summarized below:

Parabolic Trough Solar Collector average thermal input =2.3 kW

Charging duration t_{charge}= 6 h = 21,600 s.

Q_{input} = 2.3 × 6 = 16.8 kWh = 60.48 MJ

Total thermal energy Q_{stored}≈ 29.4 MJ

Useful heat recovered during discharge process ≈ 24 MJ

Reference ambient (T0 = 303 K (30 °C).

Charging Efficiency:

$$\eta_{charge} = \frac{Q_{stored}}{Q_{input}} = \frac{29.4}{60.48} = 0.486 = 48.6\ \%$$

Discharging Efficiency:

$$\eta_{discharge} = \frac{Q_{useful}}{Q_{stored}} = \frac{24}{29.4} = 0.816 = 81.6\ \%$$

Round-trip Efficiency

$$\eta_{RT} = \eta_{charge} \times \eta_{discharge} = 0.486 \times 0.816$$

$$= 0.396 = 39.6\ \%$$

The high discharging efficiency demonstrates the powerful heat retention capacity of thermal storage material (solar salt), whereas the comparatively poor charging efficiency is mostly caused by optical and thermal losses in the PTC and circulation loop.

4. CONCLUSION

This research experimentally evaluated the thermal efficiency of a Solar salt-based thermal energy storage system charged by a parabolic trough solar collector and functioning with a graphene–TiO_2/ethylene glycol hybrid nanofluid as the heat transfer medium. Experiments involving outdoor charging and regulated discharging were performed to evaluate temperature distribution, heat retention characteristics, and overall system performance under laboratory-scale operating conditions.

The findings indicate that the hybrid nanofluid enhances heat transfer in the charging phase, facilitates a more consistent temperature distribution within the storage tank near the melting temperature of solar salt, and contributes to prolonged and steadier heat-release duration during discharging. The system demonstrated a charging efficiency of 48.6%, a discharging efficiency of 81.6%, and a round-trip efficiency of 39.6%, with losses mainly due to optical and thermal inefficiencies in the solar collector and circulation loop. Although the research focuses on a laboratory-scale outdoor configuration, the experimental findings suggest that hybrid nanofluid-assisted heat transfer can enhance thermal management in molten-salt-based TES systems. These results offer valuable experimental insights for the advancement and additional assessment of improved thermal energy storage ideas for concentrated solar power uses.

FUNDING

This research received no specific grant from any funding agency in the public, commercial, or not-for-profit sectors.

CONFLICTS OF INTEREST

The authors declare that there are no conflicts of interest.

COPYRIGHT

This article is an open-access article distributed under the terms and conditions of the Creative Commons Attribution (CC BY) license (http://creativecommons.org/licenses/by/4.0/).



REFERENCES

Abbas, N., Awan, M. B., Amer, M., Ammar, S. M., Sajjad, U., Ali, H. M., Zahra, N., Hussain, M., Badshah, M. A. and Jafry, A. T., Applications of nanofluids in photovoltaic thermal systems: A review of recent advances, *Phys. A Stat. Mech. Appl.*, 536, 122513 (2019). https://doi.org/10.1016/j.physa.2019.122513

Alhamayani, A., Performance analysis and machine learning algorithms of parabolic trough solar collectors using Al_2O_3–MWCNT as a hybrid nanofluid, *Case Stud. Therm. Eng.*, 57, 104321 (2024). https://doi.org/10.1016/j.csite.2024.104321

Alhamayani, A. and Al-lehaibi, M., The effect of adding hybrid nanoparticles (Al_2O_3–TiO_2) on the performance of parabolic trough solar collectors using different thermal oils and molten salts, *Case Stud. Therm. Eng.*, 59, 104593 (2024). https://doi.org/10.1016/j.csite.2024.104593

Al-Rabeeah, A. Y., Seres, I. and Farkas, I., Experimental and numerical investigation of parabolic trough solar collector thermal efficiency enhanced by graphene–Fe_3O_4/water hybrid nanofluid, *Res. Eng.*, 21, 101887 (2024). https://doi.org/10.1016/j.rineng.2024.101887

Alva, G., Liu, L., Huang, X. and Fang, G., Thermal energy storage materials and systems for solar energy applications: A review, *Renew. Sustain. Energy Rev.*, 68, 693–706 (2017). https://doi.org/10.1016/j.rser.2016.10.021

Bellos, E. and Tzivanidis, C., Optimization of a solar-driven trigeneration system with nanofluid-based parabolic trough collectors, *Energies*, 10(7), 848 (2017). https://doi.org/10.3390/en10070848

Bellos, E., Tzivanidis, C. and Tsimpoukis, D., Enhancing the performance of parabolic trough collectors using nanofluids and turbulators, *Renew. Sustain. Energy Rev.*, 91, 358–375 (2018). https://doi.org/10.1016/j.rser.2018.03.091

Bradshaw, R. W. and Meeker, D. E., High-temperature stability of ternary nitrate molten salts for solar thermal energy systems, *Sol. Energy Mater.*, 21(1), 51–60 (1990). https://doi.org/10.1016/0165-1633(90)90042-Y

Brahim, T. and Jemni, A., Comparative study of parabolic trough solar collector using Syslltherm-800 and Therminol-VP1 non-metallic nanofluids, *Therm. Sci. Eng. Prog.*, 43, 101951 (2023). https://doi.org/10.1016/j.tsep.2023.101951

Cascetta, M., Petrollese, M., Oyekale, J. and Cau, G., Thermocline vs. two-tank direct thermal storage system for concentrating solar power plants: A comparative techno-economic assessment, *Int. J. Energy Res.*, 45, 17721–17737 (2021). https://doi.org/10.1002/er.7005

Eastman, J. A., Choi, U. S., Li, S., Thompson, L. J. and Lee, S., Enhanced Thermal Conductivity through the Development of Nanofluids, *MRS Online Proc. Libr.,* 457, 3–11 (1996). https://doi.org/10.1557/PROC-457-3

Esmaeili, Z., Akbarzadeh, S., Rashidi, S. and Valipour, M.S., Effects of hybrid nanofluids and turbulator on efficiency improvement of parabolic trough solar collectors, *Eng. Anal. Bound. Elem.*, 148, 114–125 (2023). https://doi.org/10.1016/j.enganabound.2022.12.024

Ghasemi, S. E. and Ranjbar, A. A., Effect of using nanofluids on efficiency of parabolic trough collectors in solar thermal electric power plants, *Int. J. Hydrogen Energy*, 42, 21626–21634 (2017). https://doi.org/10.1016/j.ijhydene.2017.07.087

Gil, A., Medrano, M., Martorell, I., Lázaro, A., Dolado, P., Zalba, B. and Cabeza, L. F., State of the art on high temperature thermal energy storage for power generation, *Renew. Sustain. Energy Rev.*, 14(1), 31–55 (2010). https://doi.org/10.1016/j.rser.2009.07.035

Heyhat, M. M., Valizade, M., Abdolahzade, S. and Maerefat, M., Thermal efficiency enhancement of direct absorption parabolic trough solar collector (DAPTSC) by using nanofluid and metal foam, *Energy*, 192, 116662 (2020). https://doi.org/10.1016/j.energy.2019.116662

Huang, W. and Marefati, M., Energy, exergy, environmental and economic comparison of various solar thermal systems using water and Thermia oil B base fluids, and CuO and Al_2O_3 nanofluids, *Energy Rep.*, 6, 2919–2947 (2020). https://doi.org/10.1016/j.egyr.2020.10.021

Kuravi, S., Trahan, J., Goswami, D. Y., Rahman, M. M. and Stefanakos, E. K., Thermal energy storage technologies and systems for concentrating solar power plants, *Prog. Energy Combust. Sci.*, 39(4), 285–319 (2013). https://doi.org/10.1016/j.pecs.2013.02.001

Loni, R., Askari Asli-Ardeh, E., Ghobadian, B., Kasaeian, A. B. and Bellos, E., Thermal performance comparison between Al_2O_3/oil and SiO_2/oil nanofluids in cylindrical cavity receiver based on experimental study, *Renew. Energy*, 129, 652–665 (2018). https://doi.org/10.1016/j.renene.2018.06.029

Mahian, O., Kianifar, A., Kalogirou, S. A., Pop, I. and Wongwises, S., A review of the applications of nanofluids in solar energy, *Int. J. Heat Mass Trans.*, 57(2), 582–594 (2013). https://doi.org/10.1016/j.ijheatmasstransfer.2012.10.037

Rajagopal, M., Upcycling end-of-life EV batteries into modular latent heat storage units for sustainable district heating, *Next Res.*, 2, 100819 (2025). https://doi.org/10.1016/j.nexres.2025.100819

Rajendran, D. R., Sundaram, E. G. and Jawahar, P., Experimental studies on the effect of enhanced thermal conductivity of SiC+water nanofluid in the performance of small scale solar parabolic dish receiver, *Int. J. Nanosci.*, 17, 1760025 (2018). https://doi.org/10.1142/S0219581X17600250

Ram, S., Ganesan, H., Saini, V. and Kumar, A., Performance assessment of a parabolic trough solar collector using nanofluid and water based on direct absorption, *Renew. Energy*, 214, 11–22 (2023). https://doi.org/10.1016/j.renene.2023.06.016

Saidur, R., Leong, K. Y. and Mohammad, H. A., A review on applications and challenges of nanofluids. *Renew. Sustain. Energy Rev.*, 15(3), 1646–1668 (2011). https://doi.org/10.1016/j.rser.2010.11.035

Suresh, S., Venkitaraj, K. P., Selvakumar, P., and Chandrasekar, M., Synthesis of Al_2O_3–Cu/water hybrid nanofluids using two-step method and its thermo-physical properties. *Colloids Surf. A Physicochem. Eng. Asp*., 388(1–3), 41–48 (2012). https://doi.org/10.1016/j.colsurfa.2011.08.005

Taylor, R. A., Phelan, P. E., Otanicar, T. P., Walker, C. A., Nguyen, M., Trimble, S. and Prasher, R., Applicability of nanofluids in high flux solar collectors, *J. Renew. Sustain. Energy*, 3, 023104 (2011). https://doi.org/10.1063/1.3571565

Xiong, Q., Hajjar, A., Alshuraiaan, B., Izadi, M., Altnji, S. and Shehzad, S. A., State-of-the-art review of nanofluids in solar collectors: A review based on the type of the dispersed nanoparticles, *J. Clean. Prod.*, 310, 127528 (2021). https://doi.org/10.1016/j.jclepro.2021.127528